Available online at www.sciencedirect.com
ScienceDirect
International Journal of Thermal Sciences 48 (2009) 342–352
International Journal of Thermal Sciences
www.elsevier.com/locate/ijts

Constructal tree-shaped microchannel networks for maximizing the saturated critical heat flux

Rémi Revellin [a,*], John R. Thome [b], Adrian Bejan [c], Jocelyn Bonjour [a]

[a] *Centre de Thermique de Lyon (CETHIL), UMR 5008 CNRS-INSA-Univ. Lyon 1, Bât. Sadi Carnot, INSA-Lyon, F-69621 Villeurbanne Cedex, France*
[b] *École Polytechnique Fédérale de Lausanne, STI ISE LTCM, ME G1 464, Station 9, CH-1015 Lausanne, Switzerland*
[c] *Department of Mechanical Engineering and Materials Science, Duke University, Durham, NC 27708-0300, USA*

Received 10 September 2007; received in revised form 27 May 2008; accepted 15 June 2008

Available online 29 July 2008

Abstract

A constructal tree-shaped microchannel network for maximizing the saturated critical heat flux in a disc-shaped planar body has been investigated. n_0 radial channels touch the center and n_p channels touch the periphery. Designs with no pairing level ($n_0 = n_p$), one pairing level ($2n_0 = n_p$) and two pairing levels ($4n_0 = n_p$) have been studied. The fluid simulated is R-134a at a saturation temperature of $T_{sat} = 30\,^{\circ}\mathrm{C}$ with no inlet subcooling. The flow enters at the center and exits at the periphery. The theoretical CHF model of Revellin and Thome [R. Revellin, J.R. Thome, A theoretical model for the prediction of the critical heat flux in heated microchannels, Int. J. Heat Mass Transfer 51 (2008) 1216–1225], specially developed for micro and minichannels, has been modified and used for predicting the wall CHF of low pressure refrigerants flowing in microchannels. The constraints are the disc radius R and the total volume of ducts V. The degrees of freedom are n_0, n_p and the mass flow rate $\dot{m}$. In each case, the minimum global fluid flow resistance design has been adopted as proposed by Wechsatol et al. [W. Wechsatol, S. Lorente, A. Bejan, Optimal tree-shaped networks for fluid flow in a disc-shaped body, Int. J. Heat Mass Transfer 45 (2002) 4911–4924]. Maximizing the base CHF means increasing the number of central tubes for a given complexity. Furthermore, it is better to use a simple radial structure (with no pairing level) and $2n_0$ central tubes than a design with one pairing level and n_0 central tubes. On one hand, simplified structures seem to be roughly better for maximizing the base CHF. On the other hand, coupling the base CHF and the pumping power leads to different conclusions. There exists an optimal n_0 and n_p to maximize the base CHF for each range of pumping power. For instance, for low pumping power, using radial ducts without pairing level is the best solution for dissipating high base CHF whereas for higher pumping power, a more complex design is beneficial with greater n_p. In conclusion, the recommended complexity is modest (not maximal), and high complexity is not necessarily the best solution.

Keywords: Critical heat flux; Microchannel; Flow boiling; Refrigerant; Chip cooling; Constructal; Dendritic

1. Introduction

Cooling of microprocessors and power electronics become an important issue in electronics. During the last decades various ways have been investigated to dissipate high heat fluxes (up to 3000 $\mathrm{kW/m^2}$). Flow boiling in multi-microchannel evaporators of low pressure refrigerants is one of the most promising solutions to dissipate such high heat fluxes. The upper operational limit of a micro-evaporator cooling element is the critical heat flux (CHF). It is the maximum heat flux that can be dissipated by an evaporating two-phase flow without a large excursion in wall temperature. It refers to the replacement of the liquid being in contact with the heated surface with a vapor blanket. The thermal conductivity of the vapor is very low compared to that of the liquid, and the heat transfer coefficient drops dramatically, resulting in the sudden increase of the surface temperature and possible failure of the cooled device.

The objective here is to combine constructal theory of Bejan [3] to the CHF theory of Revellin and Thome [4] (a CHF model specially developed for flow boiling of refrigerants in micro- and minichannels) in order to analyze the possible benefits for high heat flux cooling using boiling in microchannels. The Constructal Law states that for a finite-size flow system to

* Corresponding author. Tel.: +33 4 72 43 83 46; fax: +33 4 72 43 88 11.
E-mail address: remi.revellin@insa-lyon.fr (R. Revellin).

1290-0729/$ – see front matter
doi:10.1016/j.ijthermalsci.2008.06.009

Nomenclature

A	cross sectional area	m^2
C	complexity	
c_p	specific heat at constant pressure	J/kg K
CHF	critical heat flux	W/m^2
dz	element of discretization	m
D	channel diameter	m
g	acceleration of gravity	m/s^2
G	mass flux	kg/m^2 s
h_{lv}	latent heat of vaporization	J/kg
L	length	m
$\dot{m}$	mass flow	kg/s
n_0	number of central channels	
n_p	number of peripheral channels	
p	pressure	Pa
P	perimeter of the channel	m
q	base heat flux	W/m^2
q_α	base heat flux of the sector α	W/m^2
q_w	wall heat flux	W/m^2
r	radius of the vapor core	m
R	disc radius	m
Re	Reynolds number	
T	temperature	°C
u	velocity	m/s
V	total channel flow volume	m^3
We	Weber number	
x	vapor quality	
z	length along channel from entrance	m

Greek letters

α	angle	rad
β	angle	rad
γ	angle	rad
Γ	diameter ratio	
δ	film thickness	μm
Δ	difference	
$\Delta\delta_i$	height of the interfacial waves	μm
μ	dynamic viscosity	Pa s
ξ	CHF ratio	
ρ	density	kg/m^3
σ	surface tension	N/m
τ	shear stress	N/m^2
Υ	geometrical parameter	

Subscripts

b	base
int	interfacial
l	liquid
lo	liquid only
min	minimum
sat	saturation
sub	subcooling
v	vapor
w	wall

persist in time (to live), it must evolve in such a way that it provides easier access to the imposed (global) currents that flow through it. This law states that if a system is free to morph under global constraints, the better flow architecture is the one that minimizes the global flow resistances, or maximizes the global flow access [5].

One of the most widely used empirical methods developed for predicting saturated CHF in a single channel is the Katto and Ohno [6] correlation. For most regimes, they found a linear rise in CHF with increasing liquid subcooling. For normal refrigerants their method is applicable only down to about 3.0 mm channels. Katto [7] also proposed a general correlation for predicting CHF of forced convection boiling in uniformly heated rectangular channels fed with subcooled liquid. They concluded that this CHF is nearly equal to the CHF of forced convection boiling on heated plane surfaces in a parallel flow.

Bergles and Kandlikar [8] reviewed the existing studies on critical heat flux in microchannels. They concluded at the time of their review that single-tube CHF data were not available for microchannels. For the case of parallel multichannels they noted that all the available CHF data were taken under unstable conditions. The critical condition in that case was the result of an upstream compressible fluid instability in the parallel channel, namely the Ledinegg instability. As a result, the CHF values were lower than they would be if the channel flow were kept stable by an inlet restriction at the inlet of each channel.

Wojtan et al. [9] performed a series of single-tube tests to determine the CHF in 0.509 and 0.790 mm internal diameter microchannel tubes as a function of refrigerant mass velocity, heated length, saturation temperature and inlet liquid subcooling. The refrigerants tested were R-134a and R-245fa and the heated length of the microchannel was varied from 20 and 70 mm. The results showed a strong dependence of CHF on mass velocity, heated length and microchannel diameter, but no measurable influence of small degree of liquid subcooling (2–15 °C) tested. The experimental results were compared to the CHF single-channel correlation of Katto and Ohno [6] and the multichannel correlation of Qu and Mudawar [10], showing that the correlation of Katto–Ohno predicted their microchannel data better. The correlation of Qu and Mudawar exhibited the same trends as the CHF data but significantly overpredicted them. Based on their experimental data, a new microscale version of the Katto–Ohno correlation for the prediction of wall CHF (q_w) during saturated boiling in microchannels was proposed by Wojtan et al.:

$$\frac{q_w}{G \cdot h_{lv}} = 0.437\left(\frac{\rho_v}{\rho_l}\right)^{0.073} We_{lo}^{-0.24}\left(\frac{L}{D}\right)^{-0.72} \tag{1}$$

with

$$We_{lo} = \frac{G^2 \cdot L}{\sigma \cdot \rho_l} \tag{2}$$

Revellin and Thome [4] have since developed a theoretical model for predicting CHF in microchannels. The model is based on the premise that CHF is reached when local dryout occurs during evaporation in annular flow in a uniformly heated, circular microchannel at the location where the height of the interfacial waves reaches that of the annular film's mean thickness. Many observations confirm that CHF in microchannels often occurs in annular flow, such has been observed in Wojtan et al. [9] and Revellin and Thome [11].

Agostini et al. [12] studied high heat flux flow boiling in a silicon multi-microchannel heat sink composed of 67 parallel channels, 223 μm wide, 680 μm high and with 80 μm thick fins separating the channels. The microchannel length was 20 mm. The footprint critical heat fluxes measured varied from 1120 to 2500 kW/m^2 and the wall critical heat fluxes from 219 to 522 kW/m^2 for mass velocities from 276 to 992 kg/m^2 s. Their data were predicted well by the theoretical model of Revellin and Thome [4] and the correlation of Wojtan et al. [9].

Saturated critical heat flux has been studied extensively for macrochannels but much less for microchannels. The data base currently available for flow boiling of low pressure refrigerants in microchannels is sparse. Different correlations exist for predicting the CHF in microchannels. Use of correlations has the advantage of being simple. However, correlations are limited in their range of parameters for which they have been developed and the physics is usually not well defined. Using a numerical model, such as that of Revellin and Thome, is slightly more complex but is based on physical phenomena and can be expected to work for a large range of parameters. Moreover, a non-uniform heat flux can be applied as a boundary condition in the model whereas correlations are restricted to the use of uniform heat fluxes only.

Maximizing the critical heat flux also means optimizing the design of the evaporator with respect to pressure drop and heat transfer, an aspect not apparently addressed by any previous studies except for Revellin and Thome [13] who proposed a solution for rectangular multi-microchannel cooling elements. Indeed, they proposed a premise of optimization by saying that for cooling of micro-processors, one design solution would be to place the fluid inlet at the mid-point along the length of the microchannel element and have an exit at both ends. This would take advantage of the fact that CHF increases with decreasing channel length and would allow a higher mass flux to be used while achieving the same two-phase pressure drop. Besides, different works have already been carried out on optimal tree-shaped networks for minimizing the flow and thermal resistances.

Wechsatol et al. [2] focused on the problem of how to design a flow path with minimum overall resistance between one point (O) and many points located at the periphery of the circle centered at O. They considered a laminar and fully developed single-phase flow. They showed that when the overall size of the structure grew, the best performance was provided by increasingly more complex structures. Furthermore, as the best designs become more complex, the difference between successive designs becomes small.

Wechsatol et al. [14] also developed the optimal tree-shaped flow paths for cooling a disc-shaped body by convection. The constraints were the disc size and the total volume occupied by the ducts. The single-phase flow was assumed to be hydrodynamically and thermally fully developed. Minimizing the overall thermal resistance lead to the use of a radial structure, not dendrites. Minimizing the pumping power consumption results in the use of dendrite structures. They concluded that increasing complexity is the route to higher thermal and fluid-flow performance in the limit of decreasing scales.

Optimizing a tree-shaped disc structure to maximize the critical heat flux is the current objective using an evaporating two-phase flow in microchannels applied to electronic component cooling. Minimizing the pumping power is also an important issue. The model of Revellin and Thome [4] is modified and used here to achieve this goal. The CHF model is described below. Then the CHF model is applied to different geometries. There has been only few studies on applying constructal theory to two-phase heat transfer and none to CHF. Hence, numerous assumptions are made in order to make this first effort.

2. Critical heat flux model

The theoretical model of Revellin and Thome [4] has been used here for the prediction of the maximum mean heat flux along the microchannel (q_w) taking into account a uniform axial heat flux. It is based on the dryout mechanism of the liquid film during evaporation in annular flow for refrigerants flowing at stable conditions in heated circular microchannels. Many observations confirm that CHF in microchannels occurs in annular flow, such has been observed in Wojtan et al. [9] and Revellin and Thome [11]. It is assumed in this model that the mechanism of dryout occurs when the average liquid film is greater than 0 ($\delta_l > 0$) if the interfacial waves are large enough to have their trough in contact with the wall. In such a situation, the vapor quality x is lower than unity. Neglecting any entrainment of liquid in the gas core and any potentially significant conduction effects in the wall, the model takes into account the conservation of mass and momentum, an energy balance with the wall in a one-dimensional finite volume model and the height of the interfacial waves ($\Delta\delta_i$) is predicted using an empirical expression. This model is briefly described below.

Consider an annular flow of mass flux G in a microchannel of length L, diameter D and inner perimeter of $P = \pi D$, where u_l and u_v are the liquid and vapor velocities, ρ_l is the liquid density and ρ_v is the vapor density, p_l and p_v are the liquid and vapor pressures and h_{lv} is the latent heat of vaporization. The control volume is presented in Fig. 1. The first two equations are obtained from the conservation of mass and energy:

$$\frac{d(A_l u_l)}{dz}\,dz = -\frac{q_w P}{h_{lv}\rho_l}\,dz \tag{3}$$

$$\frac{d(A_v u_v)}{dz}\,dz = \frac{q_w P}{h_{lv}\rho_v}\,dz \tag{4}$$

The conservation of momentum gives two additional equations:

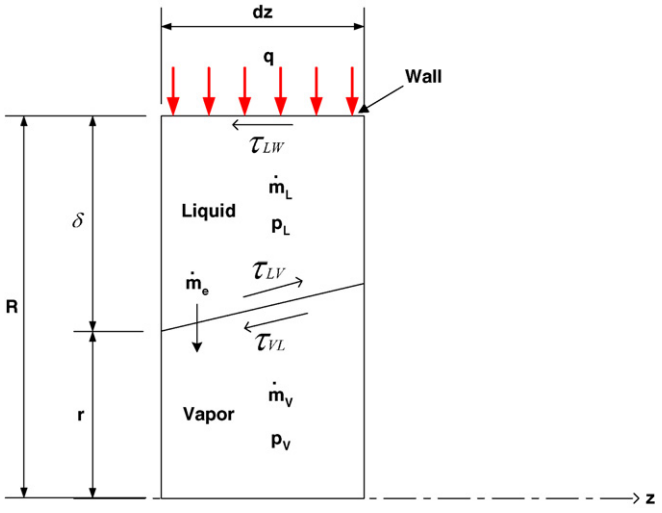

Fig. 1. Control volume of the model.

$$\rho_l \frac{d(A_l u_l^2)}{dz}\,dz = -A_l \frac{dp_l}{dz}\,dz + A_{\text{int}}|\tau_{lv}| - A_{lw}|\tau_{lw}| \tag{5}$$

$$\rho_v \frac{d(A_v u_v^2)}{dz}\,dz = -A_v \frac{dp_v}{dz}\,dz - A_{\text{int}}|\tau_{vl}| \tag{6}$$

where $A_l = \pi((D/2)^2 - r^2)$, $A_v = \pi r^2$ and $A_{\text{int}} = \pi\sqrt{2} \times (2r + dz)\,dz$ (assuming that dz has the same order of magnitude as dr) are only function of r, the radius of the vapor core. The shear stress τ_{vl} is obtained from the following equations:

$$\tau_{lv} = \frac{1}{2} C_f \rho_v u_v^2 \qquad \text{where}$$

$$C_f = \frac{16}{Re_v} \qquad \text{for } Re_v = \frac{2\rho_v u_v r}{\mu_v} < 2300$$

$$C_f = 0.078\, Re_v^{-0.25} \qquad \text{for } Re_v \geqslant 2300 \tag{7}$$

The shear stress τ_{lw} is expressed by the following relations:

$$\tau_{lw} = \frac{1}{2} C_f \rho_l u_l^2 \qquad \text{where}$$

$$C_f = \frac{16}{Re_l} \qquad \text{for } Re_l = \frac{2\rho_l u_l (D/2 - r)}{\mu_l} < 2300$$

$$C_f = 0.078\, Re_l^{-0.25} \qquad \text{for } Re_l \geqslant 2300 \tag{8}$$

The system is closed by the Laplace–Young equation for the pressure difference across the curved interface of the annular liquid film:

$$\frac{dp_v}{dz} - \frac{dp_l}{dz} = \frac{d}{dz}\left(\frac{\sigma}{r}\right) \tag{9}$$

with σ the surface tension.

The flow at the inlet at $z = 0$ is assumed to be saturated liquid. The system of 5 non-linear differential equations is solved using the fourth order Runge–Kutta method with the following boundary conditions:

$$r|_{z=0} = r_{\min}$$

$$u_v|_{z=0} = \frac{G}{\rho_l}$$

$$u_l|_{z=0} = \frac{G}{\rho_l}$$

$$p_v|_{z=0} = p_{\text{sat}}$$

$$p_l|_{z=0} = p_{\text{sat}} - \frac{\sigma}{r_{\min}} \tag{10}$$

The value of the initial radius was chosen according to Revellin and Thome [4]. The value has been set to $r_{\min} = 0.05D$.

The wall heat flux is determined by a trial-and-error process to solve for an annular liquid film thickness equal the height of the interfacial waves ($\delta_l = \Delta\delta_i$). Based on the slip ratio and the Kelvin–Helmholtz critical wavelength (assuming the film thickness to be proportional to the critical wavelength of the interfacial waves), the critical film thickness is given by the following expression:

$$\Delta\delta_i = 0.15\left(\frac{D}{2}\right)\left(\frac{u_v}{u_l}\right)^{-3/7}\left(\frac{(\rho_l - \rho_v) g (D/2)^2}{\sigma}\right)^{-1/7} \tag{11}$$

with g the acceleration of gravity.

When the equality $\delta_l = \Delta\delta_i$ is satisfied anywhere along the microchannel, CHF is reached. The adjusted constant and exponents were determined from a data base including 3 different fluids (R-134a, R-245fa and R-113), 3 different diameters (0.5, 0.8 and 3.15 mm) from experiments performed in two different laboratories [9,10].

Furthermore, this model predicts the data for circular and rectangular multi-microchannel test sections of Bowers and Mudawar [15] for R-113, and Agostini et al. [12] for R-236fa taken in a collaborative project at IBM (Switzerland) and Park and Thome for R-245fa. Agostini et al. and Park and Thome used small orifices at the inlet of each channel in order to reduce flow oscillations. The comparison between the present model and the data base (136 data) covering 4 different fluids and 7 different geometries (comprising single-microchannels and multi-circular and multi-rectangular microchannels) taken in four different laboratories is very good, predicting 91% of the data within ±20%. The mean absolute error is 10%. In the data base, the mass flux varied between 20 and 1533 kg/m^2 s for diameters ranging from 0.215 to 3.1 mm.

It is assumed here that local axial conduction effects are negligible. Such effects can be simulated on a case by case basis by coupling the present model with a finite element heat conduction solver to account for the wall material and its thickness.

Fig. 2 shows the evolution of the radius of the vapor core (δ_l) and the critical film thickness ($\Delta\delta_i$) along a microchannel. CHF occurs at the outlet of the microchannel when $\delta_l = \Delta\delta_i$.

3. Radial flow pattern

The radial flow pattern is a simple structure without pairing with as shown in Fig. 3. n_0 channels touch the center and $n_p = n_0$ channels touch the periphery. The complexity is defined as:

$$C = \frac{\ln(n_p/n_0)}{\ln(2)} \tag{12}$$

Here the complexity is 0. The flow enters at the center with a mass flow rate $\dot{m}$ and exits at the periphery ($\dot{m}_0 = \dot{m}/n_0$). This structure consists of a disc of radius R with its thickness of the order of the diameter of the channels. The disc is heated at the bottom surface with a uniform heat flux q provided by an

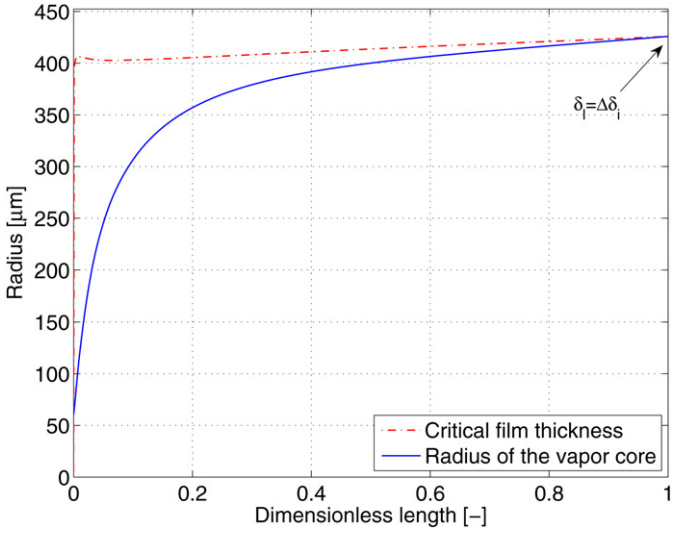

Fig. 2. Evolution of the radius of the vapor core and the critical film thickness along a microchannel with dryout a the outlet.

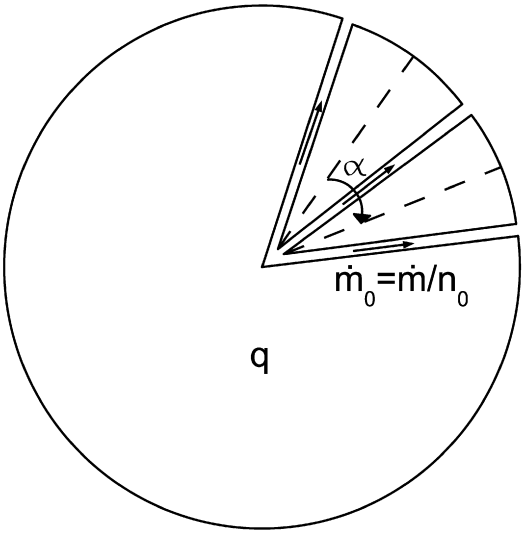

Fig. 3. Schematic of a radial flow pattern. $n_0 = n_p$.

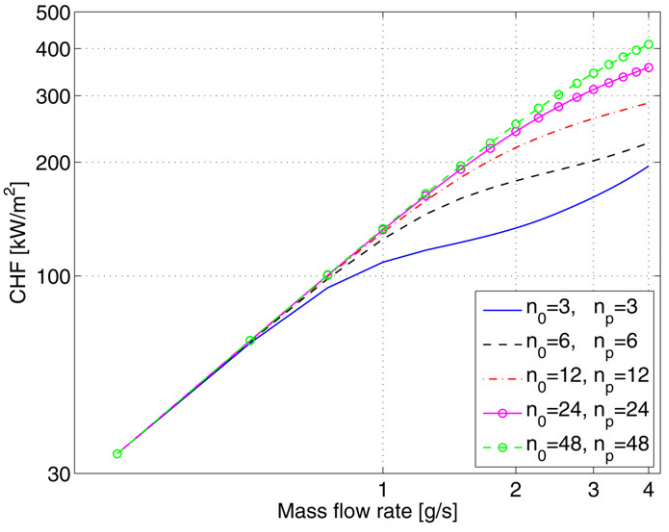

(a) Base CHF versus mass flow rate.

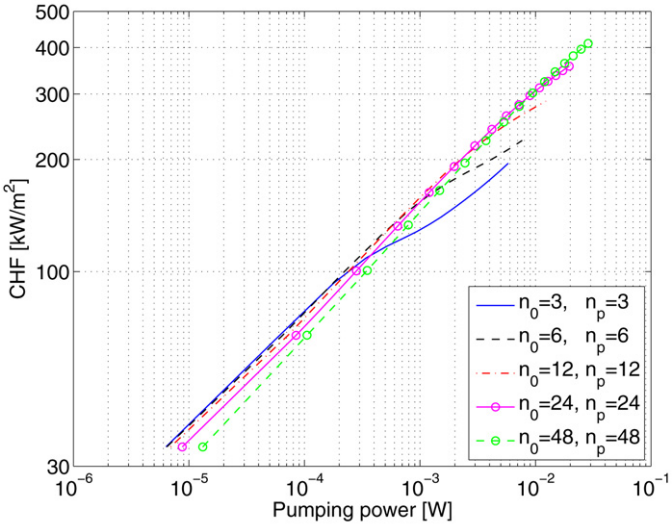

(b) Base CHF versus pumping power.

Fig. 4. Base CHF results without level pairing (radial design).

electronic component, for example. Losses are neglected and the first law of thermodynamics is applied to one sector of angle $\alpha = 2\pi/n_0$. The heat flux applied to the base of the sector ($q_\alpha = q$) is conducted uniformly toward the channel (the disk is assumed to have an infinite thermal conductivity), so we get:

$$q_w = q_\alpha \frac{2R}{n_0 D} \tag{13}$$

where q_w is the wall CHF calculated with the theoretical model. The degrees of freedom are four: R, V, n_0 (or n_p) and $\dot{m}$. The first constraint is the disc radius R and the second constraint is the constant volume of the channels defined as:

$$V = n_0 R \frac{\pi D^2}{4} \tag{14}$$

The previous relation will fix the diameter only if n_0 is known. The remaining degrees of freedom are n_0 and $\dot{m}$.

During the simulations, care was taken to stay in the domain of validity of the model, i.e. under the conditions for which the model has been experimentally validated (Section 2). The disc radius was fixed at 20 mm for the entire study and the different designs. Furthermore, the total volume of the channels V has been chosen to be close to the total volume of channels of Agostini et al. [12], i.e. 0.154 cm^3. The fluid used is R-134a at a saturation temperature of $T_{sat} = 30\,^\circ$C without any inlet subcooling.

Fig. 4(a) shows the evolution of the base critical heat flux (q_α or q) as a function of the mass flow rate ranging from 0.25 to 4.25 g/s for different values of n_0 (from 3 to 48). The higher the mass flow rate, the higher is q_α, as mentioned by Revellin and Thome [4]. For $\dot{m} = 4$ g/s, passing from $n_0 = 3$ to 48, multiplies the base CHF by 2. Furthermore, the higher n_0, the higher is q_α. According to Eq. (14), D varies like $n_0^{-1/2}$ and based on Eq. (13), q_α increases like $n_0^{1/2} q_w$. Considering the correlation of Wojtan et al. (Eq. (1)) that predicts the wall CHF of refriger-

ants in microchannels, according to this correlation, q_w varies as $D^{0.72}$ because G remains constant regardless of the value of n_0 (according to Eq. (14), $G = \dot{m}R/V$). As a result, q_α is proportional to $n_0^{0.14}$. In conclusion, we see that the increase of n_0 leads to an increase of q_α.

The present model gives also an approximate idea of the pressure drop value because it includes the calculation of the pressure gradient along the channel. The result is an approximation as it takes into account only the annular flow regime. Nevertheless, it must be recalled that this is the main flow regime encountered along the channel in case of high heat flux. This pressure drop calculation has been experimentally validated during smooth annular regime [4] but does not account for the magnifying effect of the interfacial waves. From an engineering point of view, it is useful to know either the pressure drop or the pumping power required by the system:

$$W = \frac{\dot{m}\Delta P}{\rho_l} \tag{15}$$

The base CHF versus the pumping power is presented in Fig. 4(b). For a constant pumping power, e.g., 0.005 W, it is preferable to work with a greater number of channels to increase the base CHF. However, it can be noted that there is no difference in the results for $n_0 = 24$ and $n_0 = 48$. For a pumping power of 10^{-4} W it is better to use $n_0 = 3$ ducts whereas for a pumping power of 5×10^{-4} W, $n_0 = 6$ is better. Another way to use such a graph is to consider that a fixed value of CHF is prescribed (250 kW/m^2 at the base, in the following). In that situation, what would be the best configuration to minimize the pumping power? The answer is $n_0 = 24$ or $n_0 = 48$.

We have assumed earlier that the heat flux applied to the base of the sector was conducted uniformly toward the channel assuming an infinite thermal conductivity. What if the wall heat flux is not uniformly shared out but radially distributed? The radial wall heat flux would be expressed as:

$$dq_w = q_\alpha \frac{(2\pi/n_0) r\, dr}{\pi D\, dr} = q_\alpha \frac{2r}{n_0 D} \tag{16}$$

with r the radial abscissa also corresponding to z, the length along the channel from entrance. The closer to the periphery, the higher the wall heat flux.

Fig. 5 shows the base CHF versus the mass flow rate and the pumping power for a radial distribution of the wall heat flux. Comparing with Fig. 4, a shift is observed. Indeed, the base CHF results for a radial heat flux distribution are lower than those obtained for a uniform heat flux. Nevertheless, the trends are identical and the general conclusions are not different. Thus, for a question of simplicity, a uniform wall heat flux was used for the rest of the study.

In conclusion, we can say that to aim for the highest CHF for a constant mass flow rate leads to an increase in n_0. Nevertheless, if we want to maximize the base CHF and minimize the pumping power, a more accurate study has to be performed. Furthermore, for the sake of simplicity, the inlet quality was always kept constant at $x = 0$. If the inlet condition is different, with a vapor quality greater than 0, the problem of flow maldistribution should be treated.

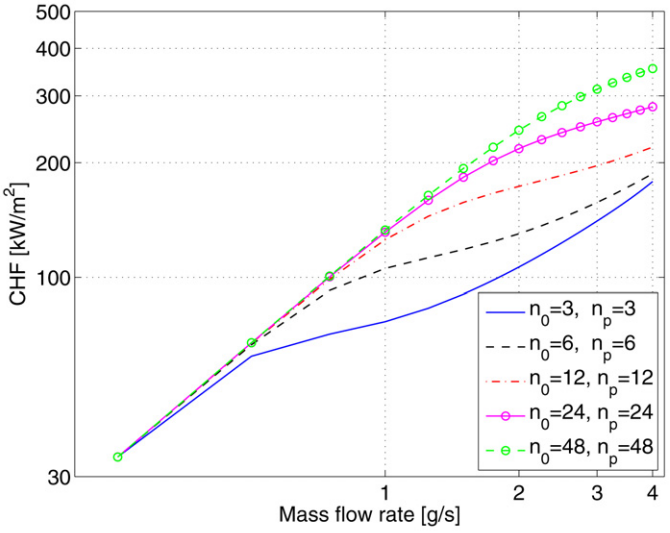

(a) Base CHF versus mass flow rate.

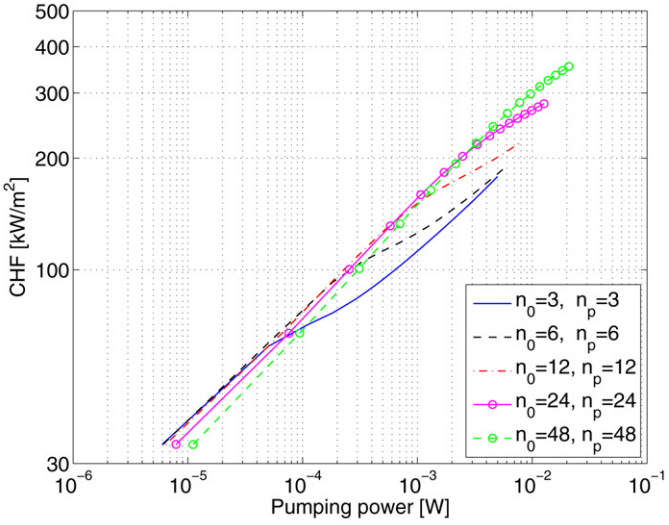

(b) Base CHF versus pumping power.

Fig. 5. Base CHF results without level pairing (radial design) for a radial wall heat flux distribution.

4. One pairing level

More complex structures are also studied here in order to evaluate the best configuration that would maximize the base CHF ($C = 1$). One pairing level is placed at the radial distance L_0 as shown in Fig. 6. n_0 channels touch the center and $n_p = 2n_0$ channels touch the periphery. L_0 and L_1 are expressed as functions of the angles α and β (as indicated in Fig. 6):

$$L_0 = R\cos\left(\frac{\alpha}{4}\right) - R\frac{\sin(\alpha/4)}{\tan(\beta)} \tag{17}$$

$$L_1 = R\frac{\sin(\alpha/4)}{\sin(\beta)} \tag{18}$$

The pairing node between the branches of level 0 and 1 is critical for the model. Knowledge of the vapor radius r, the vapor and liquid velocities (u_v and u_l) as well as the vapor and liquid pressures (p_v and p_l) is required at the beginning of each new

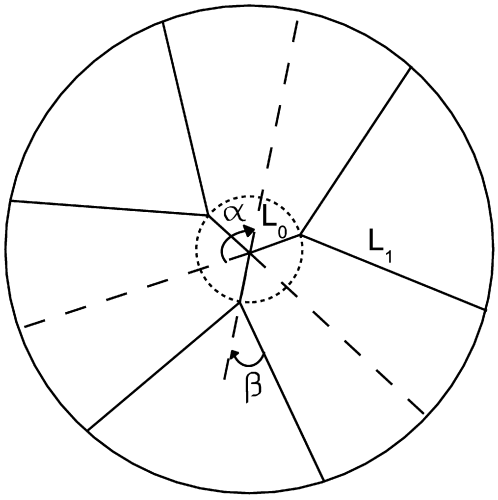

Fig. 6. Schematic of one pairing level flow pattern. $n_0 = 3$ and $n_p = 6$.

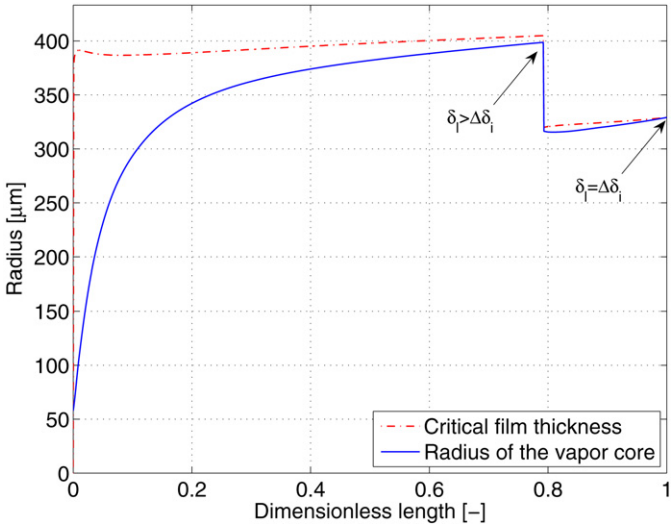

Fig. 7. Evolution of the radius of the vapor core and the critical film thickness along two successive microchannels with dryout at the outlet.

branch. For these, a conservation of void fraction is applied at the pairing node and we get for the general case:

$$\varepsilon = \frac{A_{vi}}{A_i} = \frac{A_{vi+1}}{A_{i+1}} \tag{19}$$

here $A_{vi} = \pi r_i^2$, $A_{vi+1} = \pi r_{i+1}^2$, $A_i = \pi D_i^2/4$ and $A_{i+1} = \pi D_{i+1}^2/4$, so it comes

$$r_{i+1} = r_i \frac{D_{i+1}}{D_i} = r_i \Gamma \tag{20}$$

where Γ is the ratio between the diameters of two successive channels.

Furthermore, the conservation of vapor quality at the pairing node requires:

$$x = \frac{\dot{m}_{vi}}{\dot{m}_i} = \frac{\dot{m}_{vi+1}}{\dot{m}_{i+1}} \tag{21}$$

It is assumed that the mass flow rate is equally divided in each level of branching $i+1$ ($\dot{m}_i = 2\dot{m}_{i+1}$) so that $\dot{m}_{vi} = 2\dot{m}_{vi+1}$.

Furthermore, $\dot{m}_{vi} = (\rho_v u_v A_v)_i$ and $\dot{m}_{vi+1} = (\rho_v u_v A_v)_{i+1}$, we thus obtain:

$$u_{vi+1} = \frac{1}{2} u_{vi} \Gamma^{-2} \tag{22}$$

By analogy, we get:

$$u_{li+1} = \frac{1}{2} u_{li} \Gamma^{-2} \tag{23}$$

The saturation pressure is assumed to be constant and equal to the vapor pressure so that $p_{vi} = p_{vi+1}$ and $p_{li+1} = p_{vi+1} - \sigma/r_{i+1}$ using the Laplace–Young equation. The pressure losses due to the entrance, exit and bifurcations are neglected. In view of the high pressure drops along the microchannel, these singularities would be negligible in typical small-scale applications. Besides, the final conclusions would not be changed if the singularities were taken into account, only a shift of the results would be observed.

Finally, the starting conditions used for the model at any pairing node are:

$$\begin{aligned} r_{i+1} &= r_i \Gamma \\ u_{vi+1} &= \frac{1}{2} u_{vi} \Gamma^{-2} \\ u_{li+1} &= \frac{1}{2} u_{li} \Gamma^{-2} \\ p_{vi+1} &= p_{vi} \\ p_{li+1} &= p_{vi+1} - \frac{\sigma}{r_{i+1}} \end{aligned} \tag{24}$$

As for the radial design, the heat flux applied to the base of the sector ($q_\alpha = q$) is conducted uniformly toward the channels (infinite thermal conductivity). Thus, the relation between the wall heat flux and the base heat flux is as follows:

$$q_w = q_\alpha \frac{R^2}{n_0 D_0 (L_0 + 2\Gamma L_1)} \tag{25}$$

Fig. 7 shows the evolution of the radius of the vapor core and the critical film thickness along two successive diabatic channels of length L_0 and L_1 for $\Gamma < 1$ and heated with a uniform heat flux q_w. Dryout occurs at the outlet of the second channel when $\delta_l = \Delta\delta_i$.

4.1. Diameter ratio

The value of Γ varies between 0 and 1 as the diameter decreases along the flow direction. Fig. 8 shows the influence of Γ on the base CHF for $n_0 = 24$, different mass flow rates and a constant value of β (see next section) and V. When Γ increases, the base CHF increases. At each pairing node, $G_{i+1}/G_i = \Gamma^{-2}/2$. As a result, when $\Gamma < \sqrt{1/2}$, $G_{i+1} > G_i$. We see that increasing the mass flux at the pairing node reduces the base CHF. For a value of $\Gamma > \sqrt{1/2}$, the base CHF varies slightly.

To get a better idea of the influence of Γ on the base CHF, let us consider the correlation of Wojtan et al. According to Eq. (1), the wall CHF varies as $G^{0.52} D^{0.72}$. Based on Eq. (13),

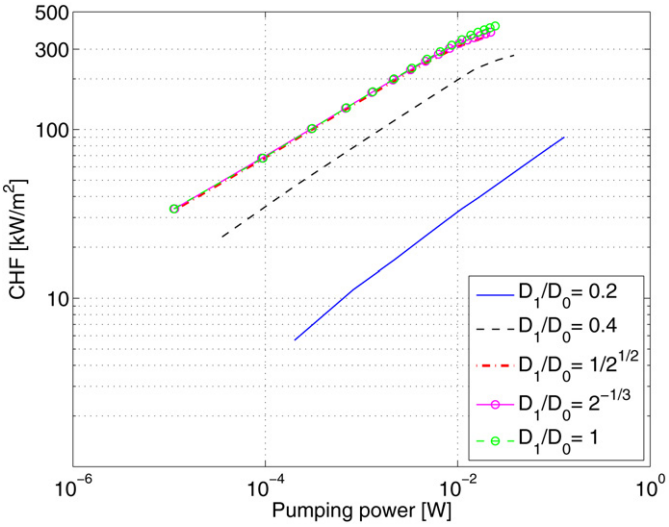

Fig. 8. Influence of the ratio between successive diameters (Γ) for one pairing level design ($n_0 = 24$).

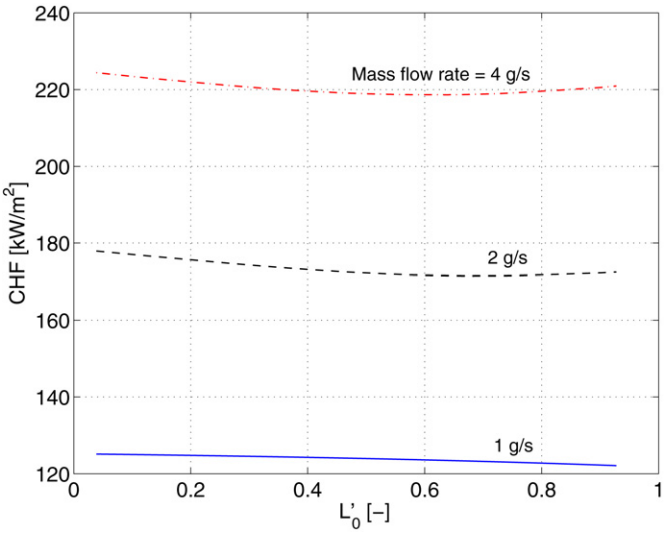

Fig. 9. Base CHF versus L_0' for a design with one pairing level and three mass flow rates ($n_0 = 3$ and $n_p = 6$).

the base CHF will vary as $G^{0.52} D^{1.72}$. The CHF is mainly controlled here by the first level of pairing as G_0 and D_0 do not vary significantly with Γ. Indeed, for $\Gamma = 0.2$, $D_0 = 0.667$ mm and $G_0 = 29.8$ kg/m^2 s and for $\Gamma = 1$, $D_0 = 0.603$ mm and $G_0 = 36.5$ kg/m^2 s. As a result, for two different values of Γ we obtain:

$$\xi = \frac{\mathrm{CHF}_{\Gamma_1}}{\mathrm{CHF}_{\Gamma_2}} = \left(\frac{\Gamma_1}{\Gamma_2}\right)^{0.68} \tag{26}$$

For $\Gamma_1 = 0.4$ and $\Gamma_2 = 1$, $\xi = 0.54$, whereas for $\Gamma_1 = 2^{-1/3}$ and $\Gamma_2 = 1$, $\xi = 1.17$. These orders of magnitude are confirmed on Fig. 8: for example, for a pumping power of 10^{-4} W, the CHF value obtained with $\Gamma = 0.4$ (35 kW/m^2) is close to that obtained for $\Gamma = 1$ (70 kW/m^2) multiplied by a factor 0.54. This approximation gives an idea of the behavior of the base CHF with Γ. The remaining question is: what is the best diameter ratio to maximize the base CHF? Usually, in single phase flow, Murray's law [3] is used ($\Gamma = 2^{-1/3}$) because many studies have shown that it was the optimal size step at each pairing node to minimize global flow resistance. Here in two-phase flow, this value is also valuable for maximizing the base CHF even if it strongly competes with $\Gamma = 1$. For the rest of the study, $\Gamma = 2^{-1/3}$ was used.

4.2. Minimum global flow resistance design

The degrees of freedom are: R, V, n_0 (or n_p), $\dot{m}$ and β. The disc radius is still fixed to R and the total volume of channels is constant and equal to:

$$V = \frac{n_0 \pi D_0^2}{4}\left(L_0 + 2\Gamma^2 L_1\right) \tag{27}$$

As a result, for each value of n_0, different geometries can be determined depending on β (or L_0 according to Eq. (17)). Fig. 9 shows the influence of $L_0' = L_0/R$ on the base CHF for different mass flow rates. The base CHF reaches a minimum for 2 and 4 g/s whereas for 1 g/s, the value of CHF decreases regularly. The highest CHF is reached for L_0' equals to 0. This value means that a radial structure without pairing level and $2n_0$ channels will be more efficient to dissipate base heat flux than a more complex design with one level pairing and n_0 central channels.

A value of β (or L_0') has to be defined at this stage to go further in the study. In order to simplify the choice, the idea is to refer to literature and use the geometry that gives the minimum global flow resistance in single phase flow as it has been performed by Wechsatol et al. [2] so that $\beta = 0.654$ rad (37.5°) is retained for the design with one level pairing.

Fig. 10(a) shows the influence of the mass flow rate and n_0 on the base CHF. As expected, the higher the mass flow rate, the higher is the base CHF. Furthermore, the greater the value of n_0 (or n_p), the higher is the base CHF. Passing from $n_0 = 3$ to 12 at $\dot{m} = 3$ g/s, multiplies the base CHF by 50%. Base CHF coupling with pumping power results gives Fig. 10(b). For $W < 10^{-4}$ W, $n_p = 3$ is the best design to maximize q_α whereas for $W = 10^{-2}$ W, $n_p = 24$ or 48 is a better choice. The conclusions are similar to those for the radial design without pairing. The objective of the highest CHF with the constraint of the lowest pumping power is not necessarily reached with a great number of radial ducts.

5. Two pairing levels

A more complex tree-shaped microchannel networks has also been studied and refers to the 2 pairing level design ($C = 2$). Fig. 11 shows an example of this structure for $n_0 = 3$ and $n_p = 12$. As explained earlier, the heat flux applied to the base of the sector ($q_\alpha = q$) is conducted uniformly toward the channels. As a consequence, the relation between the wall heat flux and the base heat flux is as follows:

$$q_w = q_\alpha \frac{R^2}{n_0 D_0 (L_0 + 2\Gamma L_1 + 4\Gamma^2 L_2)} \tag{28}$$

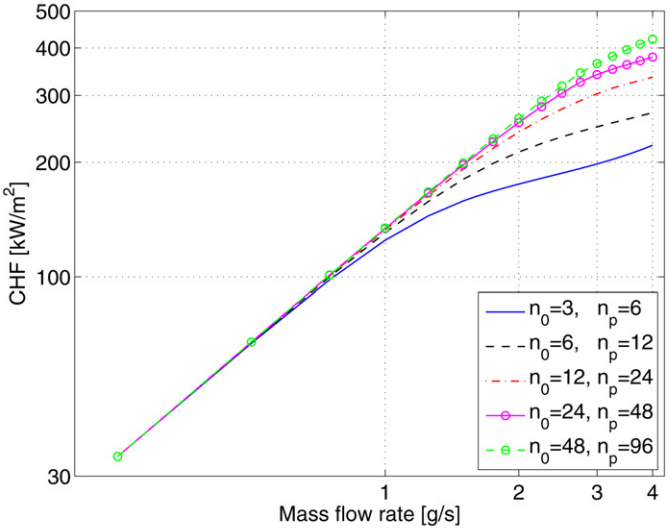

(a) Base CHF versus mass flow rate.

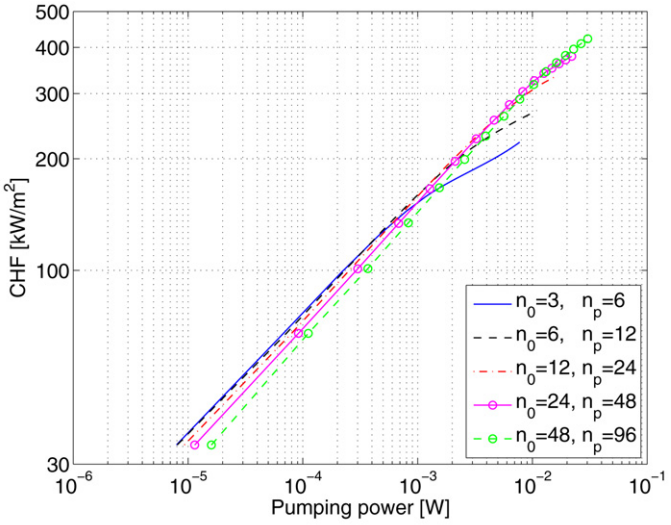

(b) Base CHF versus pumping power.

Fig. 10. Base CHF results for one level pairing in minimum global flow resistance design.

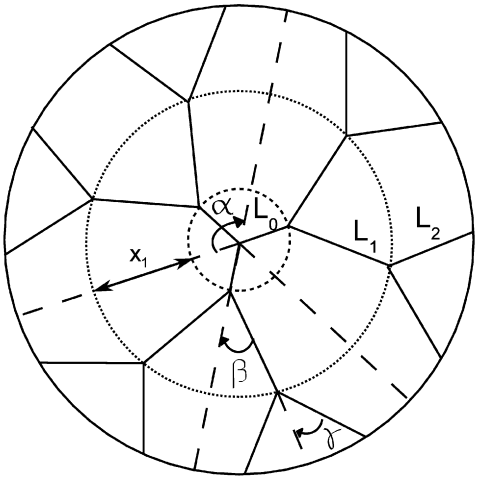

Fig. 11. Schematic of two pairing level flow pattern. $n_0 = 3$ and $n_p = 12$.

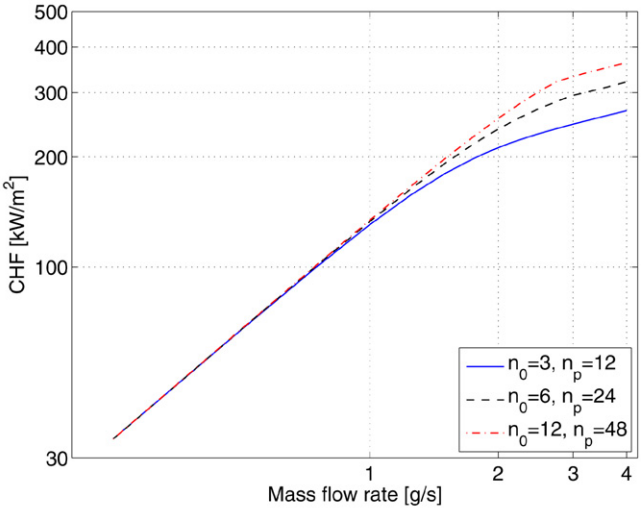

(a) Base CHF versus mass flow rate.

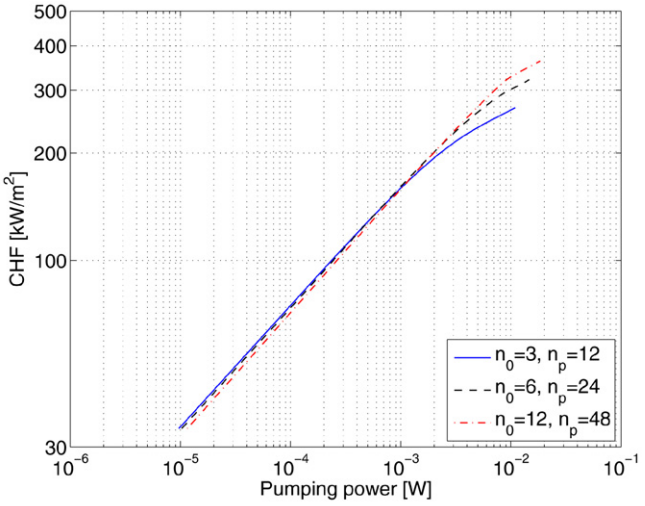

(b) Base CHF versus pumping power.

Fig. 12. Base CHF results for two level pairings in minimum global flow resistance design.

The degrees of freedom are: R, V, n_0 (or n_p), $\dot{m}$, β and γ. The constraints are the disc radius and the total volume of channels that is constant and equal to:

$$V = \frac{n_0 \pi D_0^2}{4}\left(L_0 + 2\Gamma^2 L_1 + 4\Gamma^4 L_2\right) \tag{29}$$

The design corresponds to the minimal global flow resistance of Wechsatol et al. [2]. The values of β and γ are thus fixed. L_0, L_1 and L_2 are given by the following relations:

$$L_2 = R\frac{\sin(\alpha/8)}{\sin(\gamma)} \tag{30}$$

$$L_0 = \frac{[R\cos(\alpha/8) - L_2\cos(\gamma)]\Upsilon}{1+\Upsilon} \tag{31}$$

with

$$\Upsilon = \frac{\cos(\alpha/4) - \sin(\alpha/4)/\tan(\beta)}{1 - \cos(\alpha/4) + \sin(\alpha/4)/\tan(\beta)}$$

$$L_1 = (L_0 + x_1)\frac{\sin(\alpha/4)}{\sin(\beta)} \tag{32}$$

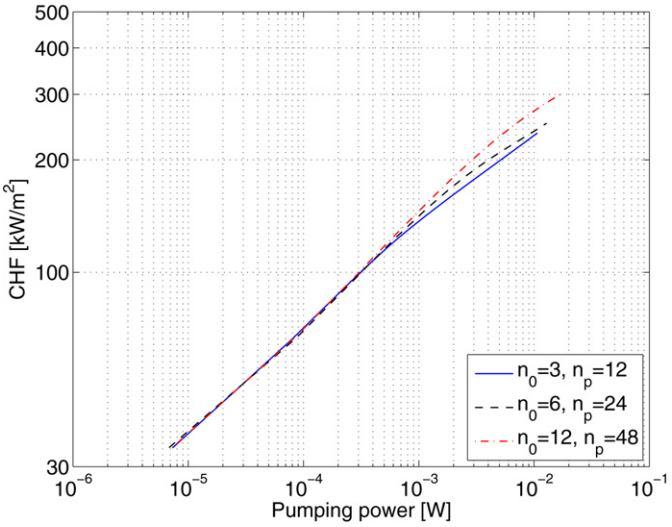

Fig. 13. Base CHF results for two level pairings in minimum global flow resistance design. The fluid enters at the periphery and exits at the center.

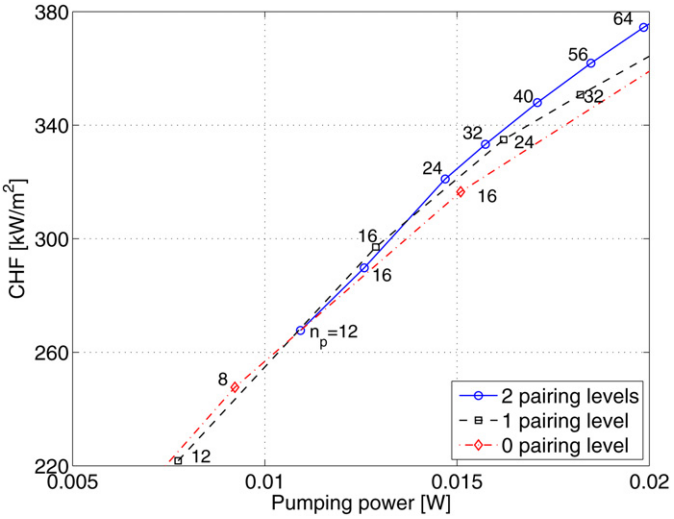

Fig. 14. CHF versus pumping power for different level pairings and $\dot{m} = 4$ g/s in minimum global flow resistance design.

with

$$x_1 = R\cos(\alpha/8) - L_0 - L_2\cos(\gamma)$$

Fig. 12(a) shows the effect of the mass flow rate (from 0.25 to 4.25 g/s) on the base CHF as well as the influence of n_0 (or n_p). As expected, the higher the mass flow rate, the higher is the base CHF. Furthermore, as previously explained, the greater the number of central channels, the higher is the base CHF. These results combined with the pumping power calculations lead to other conclusions. On Fig. 12(b) are plotted the base CHF as a function of the pumping power W for different mass flow rates and for minimal global flow resistance design. The higher the mass flow rate, the higher is the pumping power. For $W = 10^{-4}$ W, it is preferable to work with $n_0 = 3$ (or $n_p = 12$) to maximize the base CHF whereas for $W = 1.5 \times 10^{-3}$ W it is better to use $n_0 = 6$ (or $n_p = 24$). For $W = 10^{-2}$ W, the structure with $n_0 = 12$ (or $n_p = 48$) gives the highest base CHF. From an engineering point of view, increasing n_0 is not always the best solution because the pumping power is also adversely affected.

One may ask what would be the base CHF results if the fluid entered at the periphery and exited at the center. In that case, the channel diameter increases in the sense of the flow ($\Gamma = 2^{1/3}$). Fig. 13 shows the base CHF calculations as a function of the pumping power for that flow configuration. We can see that for the same pumping power, we obtain lower base CHF values than those obtained for the flow configuration of Fig. 12(b). In conclusion, entering at the center and exiting at the periphery with a decreasing diameter along the flow direction is the better solution for maximizing the base CHF.

6. Conclusions

Microprocessor cooling systems have been highly studied during the last decade because of the increasing demand of high heat flux dissipation in electronics. Using flow boiling in multi-microchannels is a very promising solution for dissipating heat fluxes up to 3000 kW/m^2 or more. As a result, experiments and modeling of two-phase flow have to be performed. For these reasons, optimization of tree-shaped microchannel networks for maximizing the saturated critical heat flux in a disc-shaped body has been investigated.

Designs with no pairing, one pairing level and two pairing levels have been studied, in which n_0 radial channels touch the center and n_p channels touch the periphery. Complexity is defined as n_p/n_0. The fluid is R-134a at a saturation temperature of $T_{sat} = 30\,^{\circ}$C without any inlet subcooling. The flow enters at the center and exits at the periphery. The theoretical CHF model of Revellin and Thome [1] (a CHF model specially developed for flow boiling of refrigerants in micro and minichannels) has been modified and used for predicting the wall CHF of low pressure refrigerants flowing in microchannels. It was assumed that all the energy applied to the bottom of the disc is uniformly conducted through the channels. The constraints are the disc radius R and the total volume of ducts V. The degrees of freedom are the number of channels touching the center n_0, the complexity (or the number of peripheral channels n_p), the mass flow rate $\dot{m}$. In each case, the minimum global fluid flow resistance design has been adopted, as proposed by Wechsatol et al. [2]. It has been shown that Murray's law is one of the best successive diameter ratio for maximizing the base CHF.

In a first approach, it is clear that increasing the number of central channels, increases the base CHF whatever is the complexity. Furthermore, it is better to use a simple radial structure (without pairing levels) with $2n_0$ central channels than a one pairing level design with n_0 central channels. Simplified structures and a greater number of central channels seem to be roughly better for maximizing the base CHF.

Analyzing the results more closely, it becomes clear that coupling the base CHF results with the pumping power leads to different conclusions. At a fixed pumping power, the highest base CHF is not necessarily reached for a greater number of channels. There exists an optimal n_0 to maximize the base CHF for each range of pumping power. Furthermore, it has been

demonstrated that the best flow configuration to maximize the base CHF is obtained for a fluid entering at the center and exiting at the periphery.

Generally, engineers need both the highest base CHF *and* the lowest pumping power to achieve an energy efficient design. Usually, the right question is: what is the design that would give the highest base CHF at the bottom of the disc-shaped body for a fixed pumping power? Fig. 14 gives an idea of how to design the tree-shaped microchannel networks. In this graph, mass flow rate has been kept constant and the minimal global flow resistance design has been adopted. For a given complexity, the greater the number of peripheral channels, the higher is the base CHF, confirming the first conclusion established in this study. Furthermore, when n_p increases, the pumping power increases for a given complexity. We also remark that increasing the complexity reduces the pumping power for a constant n_p.

Using a design with 1 pairing and $n_p = 16$ dissipates a higher base CHF than a design with 2 pairing levels and $n_p = 16$ for approximately the same pumping power. At the same time, the radial design with $n_p = n_0 = 16$ would give a higher base CHF but a higher pumping power. Furthermore, working with a 2 pairing level design with $n_p = 32$ leads to the same base CHF (335 kW/m^2) but a lower pumping power than a 1 pairing level design with $n_p = 24$. For low pumping power, let us say less than 0.01 W, using radial channels without pairing level gives the best solution for dissipating higher base CHF. High complexity is not necessarily the best. Complexity is a finite feature that must be discovered along with the rest of the flow architecture.

Finally, optimizing a tree-shaped microchannel network for maximizing the base CHF is beneficial and this topic should be pursued. Extending this study to rectangular evaporators including heat transfer resistance due to convection and conduction would be a worthwhile next step. The progress on tree-shaped constructal flow networks in several geometries was reviewed recently in [16].

References

[1] R. Revellin, J.R. Thome, A theoretical model for the prediction of the critical heat flux in heated microchannels, Int. J. Heat Mass Transfer 51 (2008) 1216–1225.
[2] W. Wechsatol, S. Lorente, A. Bejan, Optimal tree-shaped networks for fluid flow in a disc-shaped body, Int. J. Heat Mass Transfer 45 (2002) 4911–4924.
[3] A. Bejan, Shape and Structure from Engineering to Nature, Cambridge University Press, Cambridge, United Kingdom, 2000.
[4] R. Revellin, J.R. Thome, A theoretical model for the prediction of the critical heat flux in heated microchannels, Int. J. Heat Mass Transfer 51 (2008) 1216–1225.
[5] A.H. Reis, Book review, Int. J. Heat Mass Transfer 49 (2006) 445.
[6] Y. Katto, H. Ohno, An improved version of the generalized correlation of critical heat flux for the forced convective boiling in uniformly heated vertical tubes, Int. J. Heat Mass Transfer 27 (1984) 1641–1648.
[7] Y. Katto, General features of CHF of forced convection boiling in uniformly heated rectangular channels, Int. J. Heat Mass Transfer 24 (1981) 1413–1419.
[8] A.E. Bergles, S.G. Kandlikar, On the nature of critical heat flux in microchannels, J. Heat Transfer 127 (2005) 101–107.
[9] L. Wojtan, R. Revellin, J. Thome, Investigation of critical heat flux in single, uniformly heated microchannels, Exp. Thermal Fluid Sci. 30 (2006) 765–774.
[10] W. Qu, I. Mudawar, Measurement and correlation of critical heat flux in two-phase microchannel heat sinks, Int. J. Heat Mass Transfer 47 (2004) 2045–2059.
[11] R. Revellin, J.R. Thome, New type of diabatic flow pattern map for boiling heat transfer in microchannels, J. Micromechanics and Microengineering 17 (2007) 788–796.
[12] B. Agostini, R. Revellin, J.R. Thome, M. Fabbri, B. Michel, D. Calmi, U. Kloter, High heat flux flow boiling in silicon multi-microchannels: Part III. Saturated critical heat flux of R-236fa and two-phase pressure drops, Int. J. Heat Mass Transfer (2008), doi:10.1016/j.ijheatmasstransfer.2008.03.005.
[13] R. Revellin, J.R. Thome, Parametric study on CHF in flow boiling in microchannels, in: 5th International Conference on Heat Transfer, Fluid Mechanics and Thermodynamics, 1–4 July 2007, Sun City (South Africa).
[14] W. Wechsatol, S. Lorente, A. Bejan, Dendritic heat convection on a disc, Int. J. Heat Mass Transfer 46 (2003) 4381–4391.
[15] M.B. Bowers, I. Mudawar, High flux boiling in low flow rate, low pressure drop mini-channel and micro-channel heat sinks, Int. J. Heat Mass Transfer 37 (1994) 321–332.
[16] A. Bejan, S. Lorente, Constructal theory of generation of configuration in nature and engineering, J. Appl. Phys. 100 (2006) 041301.